

## Crystal optical studies of spontaneous and precursor polarization in $\text{KNbO}_3$

W. Kleemann and F. J. Schäfer

*Laboratorium für Angewandte Physik, Universität-Gesamthochschule-Duisburg, Postfach 101629,  
D-4100 Duisburg 1, Federal Republic of Germany*

M. D. Fontana

*Laboratoire de Génie Physique Equipe de Recherche associé au Centre National de la Recherche Scientifique),  
Université de Metz, Ile de Sauley, F-57045 Metz Cedex, France*

(Received 12 March 1984)

High-resolution measurements of the cubic refractive index  $n$  ( $700 \text{ K} < T < 1000 \text{ K}$ ) and of the tetragonal and orthorhombic birefringence  $\Delta n$  ( $480 \text{ K} < T < 705 \text{ K}$  and  $300 \text{ K} < T < 490 \text{ K}$ , respectively) are performed on  $\text{KNbO}_3$  in order to determine the temperature dependences of the fluctuating polarization,  $\langle P^2 \rangle$ , in the cubic phase and of the spontaneous polarization,  $P_s$ , in the ferroelectric phases. An Ornstein-Zernike analysis suggests that  $n$  is sensitive to precursor short-range order up to above  $1000 \text{ K}$  and that the fluctuating polarization, mainly due to collective order-disorder processes, reaches 58% of  $P_s = 0.33 \text{ C m}^{-2}$  at  $T_{c1} = 705 \text{ K}$ . The latter value as determined from  $\Delta n$  is 22% larger than hitherto reported. Better agreement between optically and conventionally determined  $P_s$  values is found for the orthorhombic phase.

### I. INTRODUCTION

It is well known<sup>1,2</sup> that purely displacive and order-disorder structural phase transitions (SPT's), respectively, must be considered as limiting cases which are rarely found in nature. In the case of perovskites undergoing proper ferroelectric ( $\text{BaTiO}_3$ ,  $\text{KNbO}_3$ , etc.) or improper ferroelastic SPT's ( $\text{SrTiO}_3$ ,  $\text{RbCaF}_3$ , etc.), it is widely accepted that order-disorder behavior becomes important near their cubic-tetragonal phase transition. Within a model allowing for local interwell tunneling of individual ions ( $\text{Ti}^{4+}$ ,  $\text{Nb}^{5+}$ ,  $\text{Ca}^{2+}$ , etc.), but also for harmonic coupling between adjacent ions,<sup>3,4</sup> a variety of seemingly contradicting observations can be explained.

Quite generally, the displacive character of the transition is reflected by the observation of the usual Cochran soft mode. On the other hand, the order-disorder behavior at  $T \gtrsim T_c$  causes correlated anisotropic displacements as evidenced, e.g., (i) by x-ray diffuse scattering [e.g.,  $\text{BaTiO}_3$ ,  $\text{KNbO}_3$ ,  $\text{KMnF}_3$ , and  $\text{NaNbO}_3$  (Ref. 5)], (ii) by the central peak in neutron scattering due to cluster-relaxation modes [e.g.,  $\text{SrTiO}_3$  (Ref. 6)], (iii) by contributions to the refractive index due to polarized precursor clusters [e.g.,  $\text{BaTiO}_3$  (Ref. 7)], and (iv) by the persistence of Raman lines being forbidden in the cubic phase [e.g.,  $\text{KNbO}_3$  (Ref. 8)].

In  $\text{KNbO}_3$  the order-disorder-like pretransitional effects are particularly large. Only very recently<sup>9</sup> has their role been elucidated and explained coherently with the competing soft-mode mechanism. On one hand, incomplete, though continuous, softening of the zone-center TO1 mode is observed upon passing the cubic-tetragonal-orthorhombic-rhombohedral sequence of SPT's ( $T_{c1} \sim 705 \text{ K}$ ,  $T_{c2} \sim 480 \text{ K}$ , and  $T_{c3} \sim 230 \text{ K}$ , respectively). On the other hand, large discrepancies between the experimental and calculated [via the Lyddane-Sachs-Teller (LST) rela-

tion] values of the dielectric constant are already found at  $T_{c1}$  and  $T_{c2}$ . The apparent disagreement can be resolved by assuming additional relaxational motions of the  $\text{Nb}^{5+}$  ions, which eventually drive these two SPT's.

This paper is devoted to a search for additional evidence in favor of the proposed SPT mechanism in  $\text{KNbO}_3$ .<sup>9</sup> Crystal optical investigations seem promising to measure the temperature dependence of the precursor clusters, at least in the cubic phase above  $T_{c1}$ . It is well known that they may give rise to "fluctuation tails" of the linear birefringence (LB) in transparent crystals, as observed in  $\text{SrTiO}_3$ ,<sup>10</sup> in fluoroperovskites,<sup>11</sup> and in  $\text{BaMnF}_4$ .<sup>12</sup> On the other hand, the anomalous temperature dependence of the index of refraction may also be used to measure precursor ordering. Obviously, for cubic systems such as  $\text{BaTiO}_3$ ,<sup>7</sup> the latter method is more appropriate. It is a drawback of the LB method that it requires small, but finite, anisotropic stress in order to provoke the crossover from the  $n=3$  (Heisenberg) to the  $n=1$  (Ising) regime.<sup>11,13</sup> Hence, despite the high accuracy of LB measurements, exact information on the extension of the precursor regime is scarcely available. It is one aim of this paper to demonstrate this drawback by comparing  $\Delta n(T)$  with accurate  $n(T)$  curves. These, on the other hand, allow the estimate of the average fluctuating polarization  $\langle P^2 \rangle^{1/2}$  in the cubic phase, which can be related to the dielectric-constant anomaly at  $T_{c1}$ .<sup>14</sup> A description of the temperature dependence of the  $n(T)$  anomaly will be performed within the Ornstein-Zernike approximation.

Another aim of this paper is to critically check former  $\Delta n(T)$  and  $n(T)$  data<sup>15</sup> and to describe the tetragonal LB within a Landau mean-field approach involving a first-order discontinuity of the order parameter at  $T_{c1}$ . The spontaneous polarization  $P_s$ , as derived under the assumption of preponderantly electro-optical origins of  $\Delta n$  will be compared with data of other authors. Using the Camlibel

pulse method, Günter<sup>16</sup> recently discovered that Triebwasser's<sup>14,17</sup> room-temperature value of  $P_s$  was about 30% too small. Similar corrections of the  $P_s$  values of the tetragonal phase<sup>17</sup> are expected<sup>16,9</sup> and are examined in our present investigation.

## II. EXPERIMENTAL PROCEDURE

Single crystals of KNbO<sub>3</sub> were grown by the floating-nucleus method.<sup>18</sup> At room temperature (orthorhombic phase), rectangular slabs with typical dimensions of  $2 \times 2 \times 0.2$  mm<sup>3</sup> with their edges orientated along the cubic  $\langle 001 \rangle$  directions were cut and polished. In order to remove internal strains due to the crystal growth and polishing procedure, the samples were annealed *in vacuo* at 1000 K prior to the optical measurements. These were carried out *in situ* and first upon cooling in order to take advantage of the strain-free virgin state. Linear birefringence was measured with a computer-controlled modulation method<sup>11</sup> at  $\lambda = 589.3$  nm. Great care was taken in controlling the sample position by means of a polarizing microscope. Owing to unavoidable thickness variations of the sample, considerable errors can arise from slight position changes, since, in KNbO<sub>3</sub>, the index of refraction ( $n_{\text{cubic}} \sim 2.35$ ) and the birefringence ( $\Delta n_{\text{tetrag}} \geq 0.15$ ) are rather large.<sup>15</sup> Hence, on a 0.2-mm-thick sample, precision of only about  $\delta(\Delta n) = 5 \times 10^{-6}$  is achieved. On the other hand, microscopic domain selection proves to be necessary in both the tetragonal and orthorhombic phases.

For the measurement of the refractive index in the cubic phase we used a birefringent Jamin-Lebedeff interferometer attached to the microscope.<sup>19</sup> This device permits the measurement of the phase retardation between one beam penetrating the sample and one beam passing the surrounding atmosphere. Both the phase-shift measurement and the microscopic position control correspond to those of the LB measurements. Index changes of the order  $\delta n \sim 10^{-6}$  are easily detected on samples only about 0.2 mm thick. The main source of error consists of slight changes of the sample position and orientation upon scanning the temperature over wide ranges. This restricts the accuracy to about  $\delta n \sim 5 \times 10^{-4}$  in the present study.

The LB jumps at  $T_{c1}$  and  $T_{c2}$  (Fig. 1) need separate checks of their absolute heights, since our very accurate measurement of the phase shift  $\Gamma$  omits an integer multiple of wavelengths,  $m\lambda$ . We thus have  $\Delta n = (m\lambda + \Gamma)/l$ , where  $m \sim 50$  for  $l \sim 0.2$  mm and  $T \sim T_{c1}$ . An independent measurement of  $\Delta n$  is based on the wavelength dependence of the light intensity transmitted by the sample being placed between crossed polarizers. Intensity minima appear at  $\lambda_N = l \Delta n / N$ , where  $N$  is an integer. Hence, from the spectral positions of adjacent minima,  $\lambda_N$  and  $\lambda_{N+1}$ , where  $\lambda_N < \lambda < \lambda_{N+1}$ , one easily obtains  $\Delta n = (\lambda_N^{-1} - \lambda_{N+1}^{-1})^{-1}/l$ . This method allows to determine the value of  $m$  with an accuracy of  $\pm 1$ . Moreover, the spectral spacing of the interference fringes reflects the single-domain quality of a given sample. Twin domains, which cause a decrease of the average LB, systematically enhance  $\Delta\lambda = \lambda_{N+1} - \lambda_N$ . For 0.2-mm-thick single domains,  $\delta\lambda$  is of the order of 10–15 nm.

Temperatures were measured with a calibrated NiCr-Ni thermocouple with a resolution of 0.01 K and an absolute error of about 0.5 K. Thermal equilibrium between the sample and the temperature sensor was achieved via heat-conducting He gas at a pressure of 0.4 bar.

## III. EXPERIMENTAL RESULTS

Figure 1 shows the temperature dependence of the LB in the temperature range between 300 and 900 K. The data are not corrected for the lattice contraction upon cooling, thus neglecting contributions of the order

$$\delta(\Delta n)/\Delta n \sim \alpha(T - T_0), \quad (1)$$

where  $\alpha = 5.1 \times 10^{-6} \text{ K}^{-1}$  is the average thermal lattice-expansion coefficient.<sup>9</sup>  $T_0 = 300$  K is the reference temperature for the sample thickness  $l_0$  involved in the optical-path difference. Hence, throughout the temperature range of interest, the error is smaller than 0.3%. Thermal hysteresis is found at both SPT's. The intervals are characterized by  $T_{c1}^- = 701.5$  K,  $T_{c1}^+ = 707.4$  K and  $T_{c2}^- = 476.9$  K,  $T_{c2}^+ = 493.7$  K, respectively, in good agreement with previous literature.<sup>15,9</sup> Only one of the three orthorhombic principal LB's could be measured, owing to large difficulties in reliably selecting single domains in that phase. It corresponds to the largest LB,  $n_z - n_x$ , according to and in essential agreement with Wiesendanger.<sup>15</sup>

Our results for the tetragonal LB, however, deviate appreciably from those reported previously.<sup>15</sup> In comparison, our jump at  $T_{c1}$  is about 45% larger, thus leading to a 20% downward jump at  $T_{c2}$ . In view of our careful, absolute  $\Delta n$  measurements (See Sec. II), we believe that superimposed, and yet invisible, twin domains must have diminished the LB in the former study.<sup>15</sup>

As will be discussed below, the LB arising below  $T_{c1}$  is proportional to the square of the order parameter,  $P_s$ . Within the well-known Landau-Devonshire approximation,<sup>17</sup> the tetragonal LB should hence be given by<sup>11</sup>

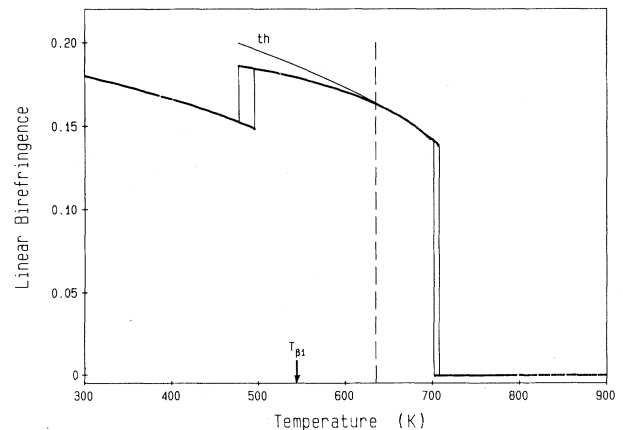


FIG. 1. Temperature dependence of the linear birefringence of cubic, tetragonal ( $|n_e - n_o|$ ), and orthorhombic ( $n_z - n_x$ ) KNbO<sub>3</sub>, respectively. Measured hysteresis is indicated by respective vertical lines. A Landau-Devonshire fit using data between  $0.9T_{c1}$  (vertical dashed line) and  $T_{c1}$  is presented as a solid line designated as "th."

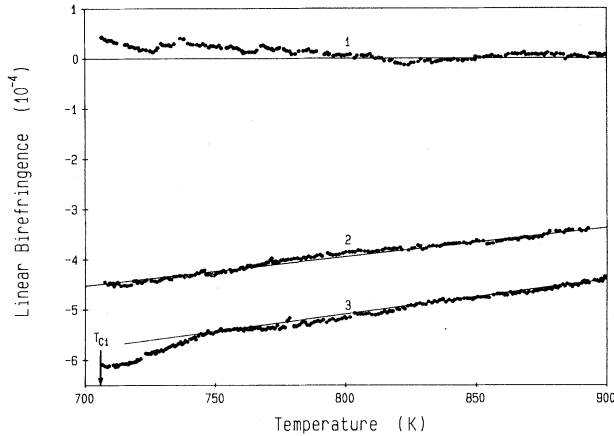


FIG. 2. Birefringence tails above  $T_{c1}$  as measured on a low-strain sample of  $\text{KNbO}_3$  at different positions. The solid straight lines refer to the regular high-temperature behavior of the strain-induced accidental birefringence.

$$\Delta n(T) = [2\Delta n(T_{c1})/3] \times \left\{ 1 + \left[ 1 - \frac{3}{4}(T - T_{\beta 1}) / (T_{c1} - T_{\beta 1}) \right]^{1/2} \right\}. \quad (2)$$

Inserting  $T_{c1} = (T_{c1}^- + 3T_{c1}^+) / 4 = 705.9$  K and  $\Delta n(T_{c1}) = 0.1398$ , a best-fit procedure involving data points within  $0.1 \leq \tau = 1 - T/T_c \leq 0.006$  yields  $T_{\beta 1} = 543.4$  K. This temperature should be (within Landau theory) identical with the divergence temperature of the susceptibility in the cubic phase,  $T_0$ . However, the Curie-Weiss law,  $\epsilon = C/(T - T_0)$ , yields values of  $T_0$  significantly higher than  $T_{\beta 1}$  [ $T_0 = 634$  K (Ref. 17) or  $T_0 = 615$  K (Ref. 20)]. This seems to hint at a failure of Eq. (2). Evidently, the calculated curve (solid line in Fig. 1, referred to as “th”) deviates from the experimental data just below  $\tau = 0.1$ , thus indicating only a poor fit, in contrast with that found for the Curie-Weiss law.<sup>17,20</sup> On one hand, Eq. (2) is, in principle, not able to accurately describe large discontinuities of the order parameter since it relies on a series expansion restricted to the sixth power of  $P_s$ . On the other hand, the proximity of the second phase transition at  $T_{c2}$  involves a coupled-order-parameter problem. This will modify the low-temperature behavior, i.e., Eq. (2), and the parameters therein, rather than the high-temperature Curie-Weiss law. In the following discussion (Sec. IV) we shall therefore use  $T_0 = 615$  K, which relies on the most recent and careful  $\epsilon$  measurements.<sup>20</sup>

The LB does not vanish completely in the cubic phase. This is shown at high resolution in Fig. 2 for one well-annealed sample probed at three different positions over areas of about  $50 \mu\text{m}^2$ . The sign of the LB is chosen such that it becomes positive in the tetragonal single domain below  $T_{c1}$ . It is remarkable that apart from positive (curve 1), negative fluctuation tails (curves 2 and 3) may also appear. Similar observations were made in our previous study<sup>11</sup> on fluoroperovskites. Local strain fields, which define an elasto-optically induced bias LB, are involved. Following our previous discussion,<sup>11</sup> it may be inferred that local [101] strain is responsible for both the creation of a future [010] single domain (“ordering mech-

anism”) and the evolution of a positive fluctuation tail. Here, we adopt the geometry of [001] being the direction of light propagation and [010] being the direction of the elongated  $\vec{c}$  axis. If, however, a larger [010] stress is superimposed, both [100]- and [001]-orientated microdomains will emerge. Among these, only [100] domains will be detected by the LB, yielding a negative sign. Only very near to  $T_{c1}$  will the Ising-type stress interaction with [101] symmetry select the unambiguous orientation of the future macroscopic [010] single domain below  $T_{c1}$ .

This qualitative discussion shows that rather complicated and competing interactions may be involved in the evolution of LB fluctuation tails. Moreover, the photoelastic bias LB is also temperature dependent, as shown by the extrapolated straight lines in Fig. 2. It may happen that these contributions are virtually zero (curve 1) or that they appear without any fluctuation tail superimposed (curve 2). A favorable case is met in the cubic LB shown in Fig. 1, which can be seen at higher resolution in Fig. 3 (curve 1). Note that this curve has been inverted in sign and magnified by a factor of 50. The photoelastic bias LB seems to be small compared with the fluctuation cusp. The separation of both contributions is, however, not unambiguous and would require measurement up to higher temperatures. The dashed bias line in Fig. 3 is only a crude guess.

Upon comparing the temperature dependences of the fluctuation tails in Figs. 2 and 3, it becomes evident that a quantitative treatment will, in general, be difficult. In our previous paper<sup>11</sup> we confined ourselves to the discussion of positive LB tails, which seem to involve simple strain symmetries. Unfortunately, in our present investigation on  $\text{KNbO}_3$ , positive LB tails were found very rarely and only with very small signals (Fig. 2, curve 1). The reason for this may be connected with anisotropic surface strains, which remain from cycling through the improper ferro-

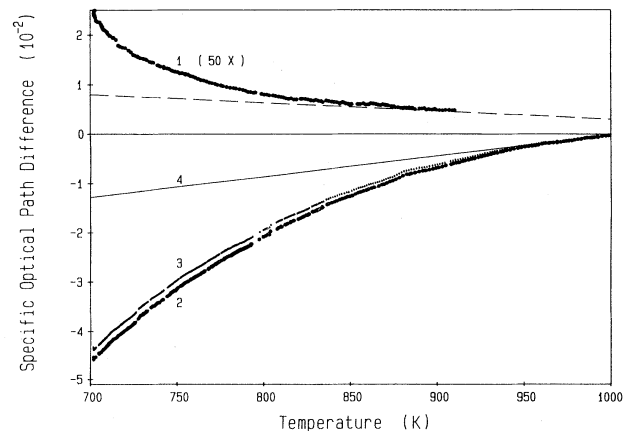


FIG. 3. Birefringence tail of a moderately strained sample of  $\text{KNbO}_3$  (curve 1 denotes magnified and inverted plot of Fig. 1 with eye-guiding dashed bias line), compared with the optical-path difference  $\Gamma(T) - \Gamma(1000 \text{ K})$  (curve 2), and with the refractive index  $n(T) - n(1000 \text{ K})$  (curve 3), respectively. Curve 4,  $n_0(T) - n_0(1000 \text{ K})$ , represents the regular part of  $n(T)$  as obtained from a best-fit linearization of curve 3 in the range  $950 < T < 1000$  K.

lastic SPT prior to the measurement.

Fortunately, it is possible to overcome these difficulties by measuring the reflective index, which is sensitive to isotropic rather than to anisotropic fluctuations. The result is shown in Fig. 3. Curve 2 denotes the variation of the specific optical-path difference,  $\Gamma/l_0$ , where  $\Gamma(T) = n(T)l(T)$  is set zero at  $T' = 1000$  K. In order to obtain the temperature dependence of  $n(T) - n(T')$  with  $n(T') = 2.36$  as extrapolated from Wiesendanger's absolute measurements,<sup>15</sup> we must correct  $\Gamma$  for the lattice expansion. In a linear approximation it is easily shown that

$$n(T) - n(T') = \Gamma(T)/l_0 - \alpha[n(T') - 1](T - T'), \quad (3)$$

which is plotted as curve 3 in Fig. 3. Extrapolating  $\alpha = 5.1 \times 10^{-6} \text{ K}^{-1}$ , as determined between 300 and 750 K up to 1000 K,<sup>9</sup> may introduce a slight error, which, however, will not seriously affect the 5% correction between curves 2 and 3.

It is seen that curve 3 in Fig. 3 deviates appreciably from a linear index of a cubic material undergoing linear lattice expansion, as usual in the high-temperature limit. It may be anticipated (see Sec. IV) that essentially all of the downward bending of the  $\delta n(T)$  curve compared with the horizontal line  $\delta n \equiv 0$  has to be attributed to the formation of precursor clusters of polarization prior to the phase transition. Hence, as in BaTiO<sub>3</sub>,<sup>7</sup> the evolution of ferroelectric short-range order can be deduced from this measurement, as will be discussed below.

#### IV. DISCUSSION

##### A. Ferroelectric short-range order in the cubic phase

As mentioned above, only limited information is available from LB tails on the fluctuation behavior of a cubic system. They require bias stress fields, which drive the system from cubic (anisotropic Heisenberg) into Ising critical behavior. Hence, data are available only below the crossover temperature, where critical behavior, if any, will be changed in a typical way.

On the other hand, the cubic refractive index is sensitive to all order-parameter fluctuations since their time constant will be large compared with the passage time,  $\tau_0 \lesssim 10^{-15}$  s, of the electromagnetic light wave through a given cluster. Hence, the light probes a statistical ensemble of quasistatic distributions of polarization clusters. Within the indicatrix description of crystal optics,<sup>21</sup> the variation of the principal dielectric impermeability components is given by

$$\delta(1/n^2)_i = \sum_{j=1}^3 g_{ij}^F P_j^2, \quad (4)$$

where the  $g_{ij}^F$  are the free electro-optic coefficients. They include photoelastic contributions due to electrostriction. Keeping in mind that we measure time- and space-averaged values  $\langle P_j^2 \rangle \equiv \langle P^2 \rangle$ ,  $j=1, 2$ , and  $3$ , and evaluating Eq. (4) as in the case of photoelasticity,<sup>21</sup> we obtain  $n(T) = n_0(T) - \delta n(T)$  with

$$\delta n(T) = (n_0^3/2)(g_{11}^F + 2g_{12}^F)\langle P^2 \rangle, \quad (5)$$

where  $n_0(T)$  is the unperturbed high-temperature refractive index. This, expected<sup>7</sup> to vary linearly with  $T$ , may be deduced from a least-squares fit of our  $n(T)$  data (Fig. 3, curve 3) in the temperature range  $950 \leq T \leq 1000$  K, as shown by the straight line (curve 4) in Fig. 3. We thus assume that the temperature dependence of  $\delta n(T)$  essentially vanishes above 950 K.

The slope of curve 4,  $dn_0/dT = 4.2 \times 10^{-5} \text{ K}^{-1}$ , must be taken as an approximate value since true linearity will be achieved only asymptotically at temperatures which lie outside of our experimental possibilities. Unfortunately, theoretical predictions of  $dn_0/dT$  are even less reliable since only the contribution due to linear lattice expansion (coefficient  $\alpha$ ) and to its coupling with the refractive index (elasto-optic coefficients  $p_{11}$  and  $p_{12}$ ) can be given explicitly. From the density dependence of the refractive index,<sup>21</sup>

$$\rho(dn_0/d\rho) = (n_0^3/6)(p_{11} + 2p_{12}), \quad (6)$$

one may deduce the "thermoelastic" contribution to  $dn_0/dT$ ,

$$(dn_0/dT)_\alpha = -(n_0^3/2)(p_{11} + 2p_{12})\alpha. \quad (7)$$

Apart from this negative contribution, which seems to dominate, e.g., in BaTiO<sub>3</sub>,<sup>7</sup> "thermo-optic" contributions of either sign may additionally be involved. These are shown to be positive and dominating, e.g., in PbTiO<sub>3</sub>,<sup>22</sup> and, seemingly, in the present case, KNbO<sub>3</sub>. They are due to purely thermal effects on the electron states involved in optical dispersion. Note that Eq. (6) originally describes isothermal behavior and is thus insufficient to account for other than crystal-field effects on  $n_0$ .

Subtracting curve 3 from curve 4 of Fig. 3 we obtain the refractive-index anomaly corresponding to Eq. (5) plotted as  $\delta n(T) - \delta n(1000 \text{ K})$  in Fig. 4. In order to obtain  $\delta n(1000 \text{ K})$  and to describe the temperature dependence of  $\delta n(T)$ , we exploit the proportionality between  $\delta n$  and  $\langle P^2 \rangle$ , which is given, via the fluctuation-dissipation theorem, by

$$\langle P^2 \rangle = (k_B T / 8\pi^3) \int \chi(\vec{q}) d^3 \vec{q}. \quad (8)$$

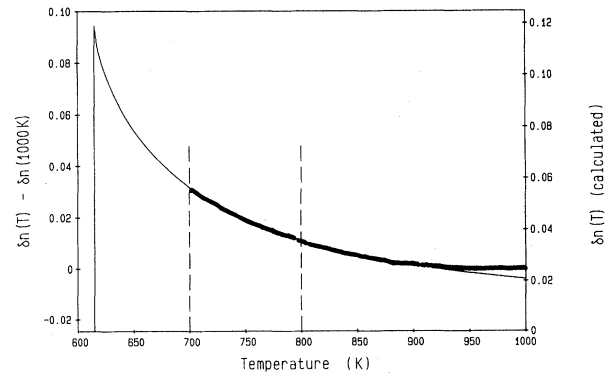


FIG. 4. Cubic refractive-index anomaly of KNbO<sub>3</sub> obtained, respectively, by subtracting curves 3 and 4 of Fig. 3,  $\delta n(T) - \delta n(1000 \text{ K})$  (dotted curve, left-hand scale), and by fitting of the data between 700 and 800 K (vertical dashed lines) to the Ornstein-Zernike expression (12),  $\delta n(T)$  (solid line, right-hand scale).

The fluctuations of the order parameter are hence determined by the  $\vec{q}$ -dependent susceptibilities  $\chi(\vec{q})$ , which may be expressed by

$$\chi(\vec{q}) = \chi(0)(1 + \xi^2 q^2)^{-1} \quad (9)$$

in the Ornstein-Zernike approximation. This relation involves the static susceptibility  $\chi(0) = \epsilon_0 \epsilon$  and the correlation length

$$\xi(t) = \xi_0 t^{-\nu}. \quad (10)$$

Using the reduced temperature  $t = T/T_0 - 1$ , where  $T_0$  is the divergence temperature of  $\epsilon$  and  $\xi$ , and the critical exponent  $\nu = 0.71$  for the three-dimensional (3D) Heisenberg model, we expect  $\xi_0$  to be of the order of the lattice constant  $a$ . It should be noted that  $\epsilon$  denotes the total dielectric constant since Eq. (4) does not discern between order-disorder and displacive (soft-mode) origins of fluctuating polarization.

Replacing the cubic Brillouin zone by a sphere with  $0 \leq q \leq q_m$ , one readily obtains

$$\langle P^2 \rangle = (k_B T \epsilon_0 q_m) [1 - \tan^{-1}(\xi q_m)/(\xi q_m)] / (2\pi^2 \xi^2). \quad (11)$$

Neglecting the temperature dependence of  $\epsilon/\xi^2 \propto t^{-\gamma+2\nu}$ , since  $\gamma \sim 2\nu$  for the 3D Heisenberg model ( $\gamma = 2\nu$  in the mean-field approximation), we thus have, from Eqs. (5) and (11),

$$\delta n(T) = c_0 T [1 - \tan^{-1}(\xi q_m)/(\xi q_m)], \quad (12)$$

with

$$c_0 = (g_{11}^F + 2g_{12}^F)(n_0^3 k_B \epsilon_0 q_m) / (\pi \xi^2). \quad (13)$$

A least-squares fit of the experimental data between  $T_{c1}$  and 800 K (Fig. 4) yields  $\delta n(1000 \text{ K}) = 0.0247$ ,  $c_0 = 1.94 \times 10^{-4}$ , and  $\xi_0 q_m = 0.45$ , if we insert  $T_0 = 615 \text{ K}$ , as obtained for pure  $\text{KNbO}_3$ .<sup>20</sup> The fit (solid line in Fig. 4) has a good correlation factor ( $r^2 = 0.9996$ ) and describes the data well up to 900 K. The deviations around 1000 K may be partially due to errors in our subtraction procedure of  $n_0(T)$  (Fig. 3, curve 4). The most important features of  $\delta n(T)$  are the typical cusp at  $T_0$  and the persistence of a finite value at 1000 K. This indicates that ferroelectric short-range order is preserved up to temperatures far above  $T_{c1}$ , as is evident from the  $\epsilon$  anomaly as well.<sup>20</sup>

Let us first calculate the value of  $\langle P^2 \rangle$  at  $T_{c1}$  from Eq. (5) using  $\delta n(T_{c1}) = 0.056$  (Fig. 4),  $n_0 = 2.36$ , and  $g_{11}^F + 2g_{12}^F = 0.23 \text{ m}^4 \text{ C}^{-2}$ .<sup>22</sup> We obtain  $\langle P^2 \rangle = 0.037 \text{ C}^2 \text{ m}^{-4}$  and thus  $\langle P^2 \rangle^{1/2} = 0.19 \text{ C m}^{-2}$ . This value indicates that the fluctuating polarization achieves about 58% of the spontaneous value,  $P_s(T_{c1}) = 0.33 \text{ C m}^{-2}$ , which is obtained from our LB data (see Sec. IV B). Hence the precursor short-range order appears to be nearly twice as large as for  $\text{BaTiO}_3$ ,<sup>7</sup> and thus underlines the order-disorder model leading to the huge  $\epsilon$  anomaly at  $T_{c1}$ .<sup>17,20</sup>

The  $\epsilon$  anomaly can be estimated using Eqs. (10) and (11), which yield

$$\epsilon(t) = \frac{2\pi^2 \xi_0^2 t^{-2\nu} \langle P^2 \rangle}{k_B T \epsilon_0 q_m [1 - \tan^{-1}(\xi q_m)/(\xi q_m)]}. \quad (14)$$

If we consider isotropic fluctuations from the entire Brillouin zone, i.e.,  $q_m = \pi/a$ , and  $\xi_0 = 0.14a$  from our best-fit parameter  $\xi_0 q_m = 0.45$ , we obtain  $\epsilon(T_{c1}) = 130$ . This value is more than 1 order of magnitude smaller than the experimental one,  $\epsilon(T_{c1}) = 3000$ .<sup>20</sup>

Possible reasons for the obvious discrepancy between theory and experiment might be due to erroneous parameters  $T_0$  and/or  $\xi_0$ , where slight changes of  $\xi_0$  are most effective [e.g., choosing  $\xi_0 = 0.4a$ , and hence  $q_m = 0.36(\pi/a)$ , yields  $\epsilon(T_{c1}) = 3000$ , if  $T_0 = 615 \text{ K}$  is maintained]. However, since we are sure that  $\delta n$  is sensitive to short-wavelength correlations (i.e.,  $q_m = \pi/a$ ), we believe instead in principal failures of our theory. These are due to the neglect of cubic anisotropy in Eq. (9), which is known<sup>5</sup> to favor correlations along  $\langle 100 \rangle$  in  $\text{KNbO}_3$ . The pretransitional clusters are correlated chains along  $\langle 100 \rangle$  extending over 10 to 100 unit cells at  $T_{c1}$ , as can be estimated from the correlation volume  $\xi^3(T_{c1})$ . Lacking data on the cubic anisotropy in  $\text{KNbO}_3$ , however, more sophisticated model calculations using the  $\delta n$  anomaly should be postponed to future investigations.

#### B. Polarization in the tetragonal and orthorhombic phases

In the tetragonal phase the LB due to electrostriction and to the polarization  $P$  is calculated within the indicatrix formalism<sup>19</sup> to become

$$\begin{aligned} \Delta n &= \delta n_3 - \delta n_1 \\ &= -(n_0^3/2)[(p_{11} - p_{12})(e_3 - e_1) + (g_{11} - g_{12})\langle P^2 \rangle]. \end{aligned} \quad (15)$$

$n_0$  denotes the high-temperature cubic index,  $e_3$  and  $e_1$  are the electrostrictive strain components, and  $p_{ij}$  ( $g_{ij}$ ) represent the elasto (electro) -optical coupling constants. Since  $(p_{11} - p_{12})(e_3 - e_1)$  is not explicitly known for  $\text{KNbO}_3$ , it is convenient to use the free  $g_{ij}^F$  coefficients instead of the clamped ones,  $g_{ij}$ . Equation (15) then becomes

$$\Delta n = -(n_0^3/2)(g_{11}^F - g_{12}^F)\langle P^2 \rangle. \quad (16)$$

The most reliable  $g_{ij}^F$  values seem to be those determined at room temperature (RT) by Günter<sup>23</sup> using his directly measured RT value  $P_s = 0.41 \text{ C m}^{-2}$ .<sup>16</sup> Based on the assumption of temperature-dependent quadratic polarization-optic coefficients,<sup>24</sup> we thus use the same values as for the fluctuation problem (see Sec. IV A). Inserting  $n_0 = 2.36$  and  $g_{11}^F - g_{12}^F = 0.20 \text{ m}^4 \text{ C}^{-2}$ , we thus have

$$\langle P^2 \rangle = 0.76 |\Delta n| \text{ C}^2 \text{ m}^{-4}. \quad (17)$$

If we neglect fluctuations below  $T_{c1}$ , which seems to be justified in view of the large drop of  $\epsilon$ , upon going from  $T_{c1}^+$  to  $T_{c1}^-$  (Ref. 20) we obtain the spontaneous polarization

$$P_s^{\text{LB}} = 0.87 |\Delta n|^{1/2} \text{ C m}^{-2}. \quad (18)$$

The right-hand side of Eq. (18), as calculated from the data of Fig. 1, is plotted versus temperature in Fig. 5. For comparison, the  $P_s$  data of Triebwasser,<sup>17</sup> obtained be-

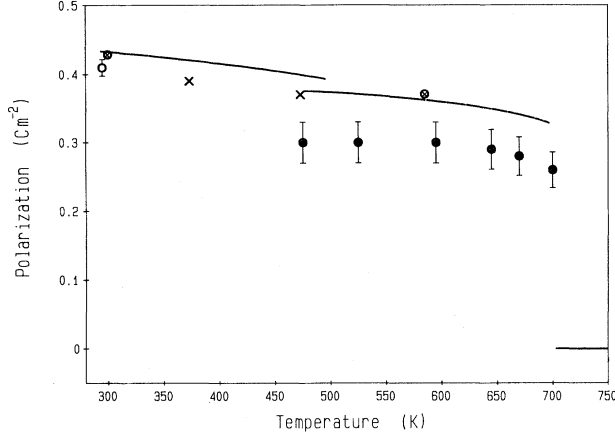


FIG. 5. Spontaneous polarization of KNbO<sub>3</sub> in its tetragonal and orthorhombic phases obtained from the birefringence curves of Fig. 1, according to Eqs. (18) and (20), respectively, in comparison with the data of Refs. 17 (●), 16 (○), 26 (×), and 9 (⊙).

tween 475 and 700 K, are also shown. It is seen that our values lie well above the 10% error margin given for  $P_s$ .<sup>17</sup> A similar 30% discrepancy was recently detected by Günter<sup>16</sup> for the room-temperature value of  $P_s$ . Recent calculations were also in favor of larger  $P_s$  values in the tetragonal phase. Values of 0.371 Cm<sup>-2</sup> (Ref. 9) and 0.396 Cm<sup>-2</sup> (Ref. 25) were suggested to replace Triebwasser's value of  $P_s=0.30$  Cm<sup>-2</sup> obtained for 500 <  $T$  < 600 K.<sup>17</sup> This is now excellently confirmed by our LB data, which yield  $P_s=0.373$  Cm<sup>-2</sup> at 500 K. It will be interesting to check this result by other experimental methods.

In the orthorhombic phase, the principal LB values are expected to be given by<sup>15,23</sup>

$$|\Delta n_{xy}| = (n_0^3/2)g_{44}^F P_s^2, \quad (19a)$$

$$|\Delta n_{yz}| = (n_0^3/4)(g_{11}^F - g_{12}^F - g_{44}^F)P_s^2, \quad (19b)$$

$$|\Delta n_{zx}| = (n_0^3/4)(g_{11}^F - g_{12}^F + g_{44}^F)P_s^2. \quad (19c)$$

Again,  $n_0$  and  $g_{ij}^F$  refer to the cubic phase.  $P_s$  is directed along the  $x$  direction in the orthorhombic or along  $[\bar{1}10]$  in the cubic coordinate frame, respectively. Since our data in Fig. 1 correspond to the largest LB (see Sec. III), the following conversion formula is readily derived from Eq. (19c):

$$P_s^{\text{LB}} = 1.02 |\Delta n_{zx}|^{1/2} \text{ Cm}^{-2}. \quad (20)$$

The corresponding curve is plotted in Fig. 5 together with  $P_s$  data measured directly at 295 K (Ref. 16) and by EPR at 373 and 473 K (Ref. 26). Moreover, comparison should be done with a calculated<sup>9</sup> value for orthorhombic KNbO<sub>3</sub>,  $P_s=0.429$  Cm<sup>-2</sup>, which fits well with  $P_s^{\text{LB}}(300 \text{ K})=0.433$  Cm<sup>-2</sup>. However, in comparison with the experimental  $P_s$  values,  $P_s^{\text{LB}}$  appears to be about 5% too large. This might indicate a systematic failure of the LB method due to "thermoelastic" contributions to  $\Delta n_{zx}$ , which arise, as for the cubic refractive index [Eq. (7)], in the following form:

$$\delta(\Delta n_{zx})_\alpha = -(n_0^3/2) \sum_{j=1}^3 (p_{3j} - p_{1j}) \alpha_j \delta T, \quad (21)$$

where the  $\alpha_j$  are the lattice-expansion coefficients. Lacking data of the orthorhombic tensor of photoelasticity, no predictions on the relevance of  $\delta(\Delta n_{zx})_\alpha$  can now be made.

### C. Latent heat at the cubic-to-tetragonal phase transition

In view of the remarkably strong short-range order appearing in the cubic phase at  $T_{c1}$  (see Sec. IV A), it seems to be interesting to estimate the jump of the entropy,  $\Delta S$ , and the latent heat,  $\Delta L$ , at  $T_{c1}$ , from our data. It was argued<sup>5</sup> that a relatively small latent heat is expected despite the strong first-order character of the transition, since the fluctuations appear to be highly correlated in the cubic phase. By integrating specific-heat curves, values of  $\Delta L=(190 \pm 15)$  and  $(135 \pm 5)$  cal/mol (Refs. 27 and 14, respectively) were obtained in former investigations. From Landau-Devonshire theory, starting with the Gibbs potential

$$G = G_0 + A(T - T_{\beta 1})P^2 + BP^4 + CP^6 - EP, \quad (22)$$

one expects, for zero electric field,<sup>17</sup>

$$\Delta L = T_{c1} \Delta S = AT_{c1} (\Delta P)^2. \quad (23)$$

Inserting their values,  $\Delta P = P_s(T_{c1}) = 0.26$  Cm<sup>-2</sup> and  $A$  from the Curie-Weiss law of  $\epsilon(T)$ , Triebwasser and Halpern<sup>14</sup> find  $\Delta L=150$  cal/mol, in reasonable agreement with the experimental values.

In view of our corrected data,  $P_s(T_{c1})=0.33$  Cm<sup>-2</sup>, the situation seems to become worse. Equation (23) now yields  $\Delta L=240$  cal/mol, which lies far from the experimental data.<sup>27,14</sup> However, a considerable amount of  $\Delta L$  is already gained above  $T_{c1}$  via the high-temperature tail of the heat capacity due to the development of short-range order. This is not accounted for in Landau theory. We thus have to correct Eq. (23) as

$$\Delta L = AT_{c1} [P_s^2(T_{c1}^-) - \langle P^2(T_{c1}^+) \rangle]. \quad (24)$$

Inserting  $\langle P^2 \rangle = 0.037$  C<sup>2</sup>m<sup>4</sup>, we now obtain  $\Delta L=159$  cal/mol, which is again in agreement with the experiments<sup>27,14</sup> and confirms the validity of our data.

## V. CONCLUSIONS

The use of electro-optical coupling constants has proved to be a powerful tool in the determination of both the spontaneous and the fluctuating polarization of KNbO<sub>3</sub> from birefringence and refractive-index measurements, respectively. For the tetragonal phase, improved values for the polarization  $P_s$  could be achieved, in agreement with predictions from experimental<sup>16</sup> and theoretical work.<sup>9,25</sup> In the cubic phase the strong deviation of  $n(T)$  from the linear law emphasizes the existence of precursor ferroelectric clusters above  $T_{c1}$ . Their persistence up to above 1000 K is in agreement with the range of discrepancy between  $\epsilon(\text{LST})$  and  $\epsilon(\text{expt})$ .<sup>9</sup> On the other hand, this feature is not inconsistent with the observation for forbidden tetragonal Raman lines<sup>8</sup> up to only  $T_{c1} + 30$  K owing to strong interference with more intense second-order lines.

It should be stressed that the detection of precursor clusters at zone-center phase transitions is particularly difficult when using "classical" scattering methods as a consequence of the superposition of the central peak with elastic or quasielastic peaks. The merits of the refractive-index method were fully recognized by Burns and Dacol<sup>7</sup> in their investigation of cubic BaTiO<sub>3</sub>, a refinement of the pioneering work of Hofmann *et al.*<sup>28</sup>. In the present work of KNbO<sub>3</sub> we have attempted to quantitatively predict not only the fluctuating polarization, but also the dielectric-constant anomaly at  $T_{c1}$ , from crystal optical data. The result is satisfying within the framework of a simple model calculation. It might be improved by taking cubic anisotropy into account.

As an outlook for future work we would like to remark that any order-parameter fluctuation as given by its autocorrelation function  $\langle \eta^2 \rangle$ , or by the susceptibilities  $\chi(\vec{q})$  via the fluctuation-dissipation theorem, should give rise to refractive-index anomalies of the kind studied in this pa-

per. The only prerequisite for its observability is its coupling to that optical-susceptibility component which transforms in the manner of the identity representation of the crystal point group.<sup>29</sup> Hence, on one hand, different contributions to  $\langle P^2 \rangle$  cannot be distinguished on principle, e.g., these may be due to relaxation modes (order-disorder mechanism) and to (nearly) soft modes (displacive mechanism), as in our present example. On the other hand, if deviations from linearity of  $n(T)$  are completely absent, as, e.g., for PbTiO<sub>3</sub> near its ferroelectric phase transition,<sup>22</sup> one must search for compensating effects. For PbTiO<sub>3</sub> one may think of the influence of hard optical modes, which transform in a way similar to  $\eta$  and which are known<sup>29</sup> to couple to the optical susceptibility as well.

#### ACKNOWLEDGMENTS

Financial support by the Deutsche Forschungsgemeinschaft is gratefully acknowledged.

- 
- <sup>1</sup>K. A. Müller, *Dynamical Critical Phenomena and Related Topics*, Vol. 104 of *Lecture Notes in Physics*, edited by C. P. Enz (Springer, Berlin, 1979), p. 210.
- <sup>2</sup>A. D. Bruce and R. A. Cowley, *Advan. Phys.* **29**, 1 (1980).
- <sup>3</sup>T. Schneider and E. Stoll, *Phys. Rev. Lett.* **31**, 1254 (1973); *Phys. Rev. B* **13**, 1216 (1976).
- <sup>4</sup>N. P. Silva, A. S. Chaves, F. C. Sà Barreto, and L. G. Ferreira, *Phys. Rev. B* **20**, 1261 (1979).
- <sup>5</sup>R. Comès, M. Lambert, and A. Guinier, *Solid State Commun.* **6**, 715 (1968); *Acta Crystallogr.* **26**, 244 (1970); R. Comès, F. Denoyer, and M. Lambert, *J. Phys. (Paris) Colloq.* **32**, C5-195 (1971).
- <sup>6</sup>T. Riste, E. J. Samuelsen, K. Otnes, and J. Feder, *Solid State Commun.* **9**, 1455 (1971).
- <sup>7</sup>G. Burns and F. H. Dacol, *Ferroelectrics* **37**, 661 (1981); *Solid State Commun.* **42**, 9 (1982).
- <sup>8</sup>M. D. Fontana, G. E. Kugel, J. Vamvakas, and C. Carabatos, *Solid State Commun.* **45**, 873 (1983).
- <sup>9</sup>M. D. Fontana, G. Métat, J. L. Servoin, and F. Gervais, *J. Phys. C* **17**, 483 (1984).
- <sup>10</sup>E. Courtens, in *Proceedings of the International School of Physics, Enrico Fermi*, Course LIX, edited by K. A. Müller and A. Rigamonti (Amsterdam, North Holland, 1976), p. 293.
- <sup>11</sup>W. Kleemann, F. J. Schäfer, and J. Nouet, *Physica* **97B**, 145 (1979).
- <sup>12</sup>F. J. Schäfer, W. Kleemann, and T. Tsuboi, *J. Phys. C* **16**, 3987 (1983).
- <sup>13</sup>G. A. Gehring, *J. Phys. C* **10**, 531 (1977).
- <sup>14</sup>S. Triebwasser and J. Halpern, *Phys. Rev.* **98**, 1562 (1955).
- <sup>15</sup>E. Wiesendanger, *Ferroelectrics* **1**, 141 (1970).
- <sup>16</sup>P. Günter, *J. Appl. Phys.* **48**, 3475 (1976).
- <sup>17</sup>S. Triebwasser, *Phys. Rev.* **101**, 993 (1956).
- <sup>18</sup>G. Métat, Ph.D. thesis, Université Lyon, (1980).
- <sup>19</sup>F. J. Schäfer and W. Kleemann, *J. Appl. Phys.* (to be published).
- <sup>20</sup>V. K. Yanovskii, *Fiz. Tverd. Tela (Leningrad)* **22**, 2201 (1980) [*Sov. Phys.—Solid State* **22**, 1284 (1980)].
- <sup>21</sup>J. F. Nye, *Physical Properties of Crystals* (Oxford University Press, Oxford, 1960), p. 245.
- <sup>22</sup>G. Burns, F. H. Dacol, J. P. Remeika, and W. Taylor, *Phys. Rev. B* **26**, 2707 (1982).
- <sup>23</sup>P. Günter, *Electro-Optics/Laser International (1976)*, edited by H. J. Gerrard (IPC Science and Technology, London, 1976), p. 121.
- <sup>24</sup>S. H. Wemple and M. di Domenico, in *Applied Solid State Science*, edited by R. Wolfe (Academic, New York, 1972), Vol. 3.
- <sup>25</sup>K. S. Kam and J. H. Henkel, *Ferroelectrics* **34**, 143 (1981).
- <sup>26</sup>F. M. Michel-Calendini, M. Peltier, and F. Micheron, *Solid State Commun.* **33**, 145 (1980).
- <sup>27</sup>G. Shirane, H. Danner, A. Pavlovic, and R. Pepinsky, *Phys. Rev.* **93**, 672 (1954).
- <sup>28</sup>R. Hofmann, S. H. Wemple, and H. Gränicher, *J. Phys. Soc. Jpn. Suppl.* **28**, 265 (1970).
- <sup>29</sup>J. Fousek and J. Petzelt, *Phys. Status Solidi A* **55**, 11 (1979).